Increased Tunneling Magnetoresistance Using Normally bcc CoFe Alloy Electrodes Made Amorphous without Glass Forming Additives

Li Gao,[1,2] Xin Jiang,[1] See-Hun Yang,[1] Philip M. Rice,[1] Teya Topuria,[1] and Stuart S. P. Parkin[1,*]

[1]*IBM Research Division, Almaden Research Center, San Jose, California 95120, USA*

[2]*Department of Applied Physics, Stanford University, Stanford, California 94305, USA*

(Received 26 January 2009; published 19 June 2009)

Using cross-section transmission electron microscopy we show that films of CoFe alloys, sandwiched between two conventional amorphous materials, are amorphous when less than ~25–30 Å thick. When these amorphous layers are integrated into magnetic tunnel junctions with amorphous alumina tunnel barriers, significantly higher tunneling magnetoresistance is found compared to when these layers are made crystalline (e.g., by heating or by thickening them). We postulate that this is likely due to changes in interfacial bonding at the alumina-CoFe interface. Indeed, x-ray emission spectroscopy shows a significant increase in the Fe, but not the Co, 3*d* density of states at the Fermi energy for thin amorphous CoFe layers.

DOI: 10.1103/PhysRevLett.102.247205 PACS numbers: 75.70.Cn, 72.25.−b, 85.75.−d

A common method to make a normally crystalline metallic material amorphous or glassy is to quench it from its liquid state [1,2]. However, most simple metals will crystallize at room temperature even at the very highest cooling rates. It is possible, in many cases, to prevent crystallization by the incorporation of small amounts of solute atoms which are either much smaller (e.g., B, C, Si) or much larger (e.g., Mo, Hf, Zr) than the host elements [2]. Recently, ferromagnetic CoFe alloys made amorphous by the addition of boron have become of especial interest because magnetic tunnel junctions (MTJs) incorporating them show the highest tunneling magnetoresistance (TMR) values at room temperature of any magnetic electrode. This is found for MTJs formed with either amorphous Al_2O_3 [3] or crystalline MgO tunnel barriers [4–7]. Whether boron plays a direct role in increasing the TMR is however unclear. Previous studies have also considered the effect of crystallization of CoFeB alloys via annealing on tunneling spin polarization and TMR [8,9], but they are complicated by the diffusion of B within the structures. Here we show that we can make normally crystalline bcc CoFe alloys amorphous without the use of any additives and that the spin polarization of the tunneling current and the associated TMR is correspondingly increased.

The films were prepared by magnetron sputtering at ambient temperature. The MTJs were patterned using *in situ* shadow masks [4]. The MTJs have a lower electrode of an exchange biased crystalline CoFe layer: 100 Ta/250 $Ir_{22}Mn_{78}$/4 $Co_{49}Fe_{21}B_{30}$/35 $Co_{70}Fe_{30}$ (thicknesses in Å), an upper electrode formed from a thin sandwiched $Co_{70}Fe_{30}$ (SCF) layer of thickness t_{SCF} inserted between an upper CoFeB (CFB) layer, 100 Å thick, and the tunnel barrier. Several different compositions of the CFB layer were used. In particular, $Co_{63}Fe_{27}B_{10}$ (CFB10) and $Co_{49}Fe_{21}B_{30}$ (CFB30) were chosen to have lower and higher crystallization temperatures, respectively, than the maximum anneal temperature T_A used in these studies (300 °C).

The structure of the SCF layer was studied with high-resolution cross-section transmission electron microscopy (XTEM). A typical micrograph is shown in Fig. 1(a) for a structure composed of five repetitions of the sequence [44 Al_2O_3/t_{SCF} SCF/100 CFB30] where t_{SCF} is 15, 20, 30, 40, and 50 Å. The structure is capped with 50 Ta/50 Ru and is deposited on 100 Ta/250 $Ir_{22}Mn_{78}$/4 $Co_{49}Fe_{21}B_{30}$/35 $Co_{70}Fe_{30}$. As can be seen clearly in Figs. 1(a) and 1(b) the SCF layer is amorphous when its thickness is $\leq$20 Å but is crystalline when $\geq$30 Å. Selected area electron diffraction shows that when the SCF layer is crystalline it exhibits a bcc structure.

Electron energy loss spectroscopy (EELS) [10] was carried out using high-resolution scanning TEM to check whether B might have diffused into the SCF layer, thereby stabilizing an amorphous state. No evidence for this was found within the spatial resolution of the EELS (~5 Å). In any case, an added complication is that the SCF does not wet the Al_2O_3 [11] layer on which it is deposited [12]. Thus the SCF grows initially as a discontinuous islanded layer, forming a continuous film only when it reaches a thickness of ~20 Å. In cross section, EELS will therefore see through portions of both the SCF and CFB layers at the boundary between these layers. However, on annealing EELS showed no change in the B profile (at 300 °C), making diffusion of B into the SCF layer during deposition at ambient temperatures unlikely.

To check whether the morphology of the SCF layer deposited on Al_2O_3 plays a role in stabilizing its amorphous structure, multilayered structures were grown in which the SCF layers are sandwiched on either side by amorphous CFB30 layers without any Al_2O_3 layers. XTEM images (not shown) indicate that the SCF layers are amorphous for thicknesses up to 20 Å and crystalline

 © 2009 The American Physical Society

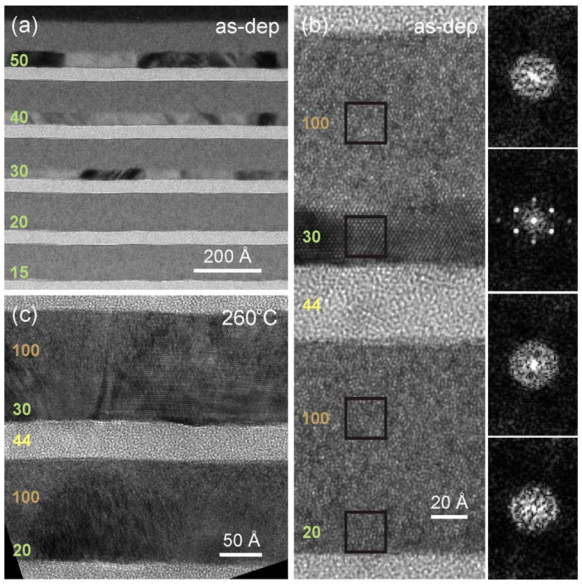

FIG. 1 (color online). High-resolution cross-section transmission electron microscopy images of 100 Ta/250 $Ir_{22}Mn_{78}$/4 $Co_{49}Fe_{21}B_{30}$/35 $Co_{70}Fe_{30}$/[44 Al_2O_3/t_{SCF} SCF/100 CFB]$_5$/50 Ta/50 Ru with t_{SCF} of 15, 20, 30, 40, and 50 Å; (a) CFB = CFB30, as deposited; (b) high magnification of a portion of (a), together with diffractograms of the four regions indicated by black square outlines in the figure. These regions are taken from (bottom to top) 20 Å SCF, 100 Å CFB30, 30 Å SCF, and 100 Å CFB30: the amorphous to crystalline transition as a function of thickness of the SCF layer is clearly revealed; (c) CFB = CFB10 annealed at 260 °C. The thicknesses (in Å) of the SCF, $A1_2O_3$, and CFB layers are labeled in green (medium gray), yellow (light gray), and orange (dark gray), respectively.

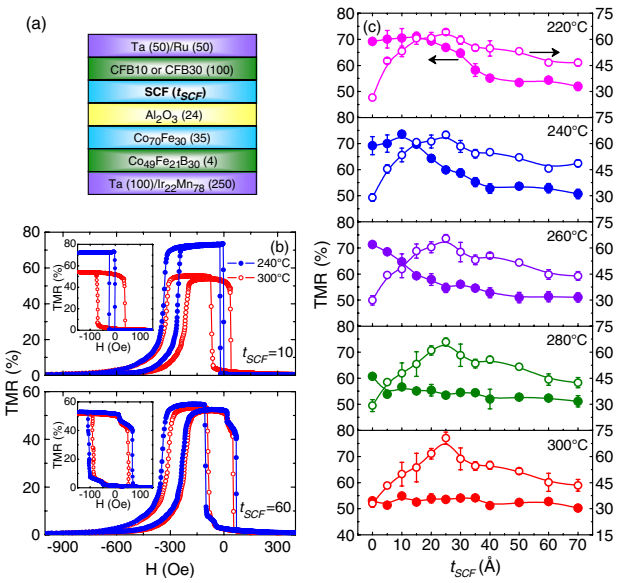

FIG. 2 (color online). (a) Schematic of the magnetic tunnel junction structure; (b) major and minor (inset) TMR loops for CFB10 samples with t_{SCF} = 10 and 60 Å; blue solid and red open circles denote results after the samples are annealed at 240 °C and 300 °C, respectively; (c) dependence of TMR on the SCF thickness at various anneal temperatures for CFB10 (solid circle) and CFB30 (open circle) samples.

for layers above 25 Å thick, a strikingly similar dependence to that for SCF layers deposited directly on Al_2O_3.

Interestingly, the CFB10 alloy has a much lower crystallization temperature than that of the CFB30 alloy so allowing its crystallization at modest temperatures. Indeed, the XTEM in Fig. 1(c) shows that the CFB10 has become crystalline after an anneal treatment at 260 °C. Moreover, this induces crystallization of the SCF layers which were previously amorphous. By contrast the CFB30 alloy remains amorphous even to 300 °C, and the thin SCF layers also remain amorphous.

Thus, we conclude that thin CoFe layers can be stabilized in an amorphous state by sandwiching them on either side by various amorphous layers, whether insulating or metallic, and that they display an amorphous to crystalline transition above a critical thickness of ~25 Å. Similar results have previously been found in Fe films grown on certain substrates at or below room temperature [13–15].

The structure of the SCF layer has an important influence on the magnetotransport properties of MTJs in which it is incorporated. Typical TMR loops are compared in Fig. 2(b) for SCF layers 10 Å and 60 Å thick. The TMR is much higher for the thinner SCF layer (~74% vs 56%). Moreover, on annealing at 300 °C, its TMR is substantially decreased and H_c is increased nearly fivefold (from ~11 Oe to 54 Oe). By contrast, the sample with the thicker SCF layer shows no significant change in either TMR or H_c for the same anneal.

The detailed anneal temperature dependence of TMR on t_{SCF} is shown in Fig. 2(c) for both CFB10 and CFB30 samples. The results are quite distinct. We first consider the case of the CFB10 alloy. The TMR shows a stepwise change from a high value for thin SCF layers to a significantly lower value for thicker layers. This transition takes place at $t_{SCF} > 20$ Å at the lowest anneal temperature of 220 °C, but with increasing T_A the transition moves to thinner SCF layers and disappears at T_A = 300 °C so that the TMR is no longer dependent on t_{SCF}. As discussed above, XTEM shows that the SCF layers, more than 15 Å thick, have become crystalline after annealing at 260 °C. Thus, we associate the change in TMR with t_{SCF} with an amorphous to crystalline transition of the SCF layer. It is reasonable to assume that the crystallization temperature depends on t_{SCF} and that thinner layers have higher crystallization temperatures, thereby accounting for the variation in the dependence of TMR with t_{SCF} on anneal temperature.

In contrast, the dependence of TMR on t_{SCF} for the CFB30 samples varies little with T_A [Fig. 2(c)]. At each anneal temperature the TMR displays a peak at t_{SCF} ~ 25 Å, and then decreases to a constant value for thicker

SCF layers. This is consistent with the XTEM results where the crystallinity of the SCF layer is not affected by annealing due to the high crystallization temperature of CFB30. Note that the initial increase in TMR with t_{SCF} is due to the low spin polarization of the high boron content CFB30 alloy and the initial islanded growth of the metallic SCF layer on the alumina layer [12].

The amorphous to crystalline transition of the SCF layer is manifested as a dramatic variation in H_c of CFB10 based MTJs, as shown in Fig. 3(a). When the SCF layer is thin and amorphous, H_c is small and independent of its thickness (see data for $T_A = 220\,^{\circ}\mathrm{C}$). However, when thin SCF layers are made crystalline by thermal annealing, H_c is increased by almost an order of magnitude (after annealing at 300 °C) and becomes similar to that of very thick SCF layers, which are crystalline as deposited. It is well known that amorphous ferromagnetic materials are magnetically soft [16]. It is also well established that H_c of thin ferromagnetic layers increases strongly with the diameter D of the crystalline grains (as $\sim D^6$) [17–20]. Thus, the dependence of H_c on t_{SCF} and on T_A is readily understood from an amorphous to crystalline transition of the SCF layer and CFB10 layer. When the SCF layer is thin, and amorphous as deposited, the entire free layer crystallizes all at the same time leading to large grains whose size will be determined by nucleation and grain growth processes within the combination of the SCF and CFB10 layers. The underlying alumina layer will play no significant role since it is amorphous. As the SCF layer is increased in thickness and crystallizes, the grain size of the as-deposited SCF layer will be limited by its comparatively small thickness (20–30 Å). (Note that the grain size of thin film layers typically varies as the layer thickness.) On annealing the CFB10 layer will crystallize but its grain size will be templated by that of the underlying crystalline SCF layer. As t_{SCF} is increased, its grain size and thus the grain size of the overlying CFB10 layer on crystallization will increase and thereby increase H_c.

The dependence of H_c on t_{SCF} for MTJs with CFB30 layers is quite similar to that with CFB10 layers annealed at the lowest anneal temperature considered (220 °C) [Fig. 3(b)]. However, there is almost no change in the dependence of H_c on t_{SCF} on annealing up to 300 °C since the CFB30 alloy remains amorphous at these anneal temperatures. Thus, we can conclude that the dependence of H_c on t_{SCF} is largely determined by the structure and grain size of the SCF layer, and that, at these comparatively low anneal temperatures, there is little grain growth during annealing.

An important question is whether the thickness of the SCF layer $t_{A\text{-}C}$ at which the amorphous to crystalline transition takes place is correlated with the thickness t_c at which the SCF layer becomes continuous [21]. t_c can be estimated from the SCF thickness at which the TMR reaches its maximum value (assuming that $t_c < t_{A\text{-}C}$). Thus, we estimate that $t_c \sim 20$–25 Å for growth of SCF on Al_2O_3 but only ~10–15 Å for growth on $Co_{40}Fe_{40}B_{20}$ [22]. Since $t_{A\text{-}C}$ is similar for SCF layers grown on insulating Al_2O_3 and metallic CFB layers, we conclude that $t_{A\text{-}C}$ is not simply related to t_c.

The dependence of TMR on T_A is summarized in Figs. 3(c) and 3(d) for free layers with representative thicknesses of 20 and 60 Å thick SCF layers for the CFB10 and CFB30 alloys, respectively. For both CFB

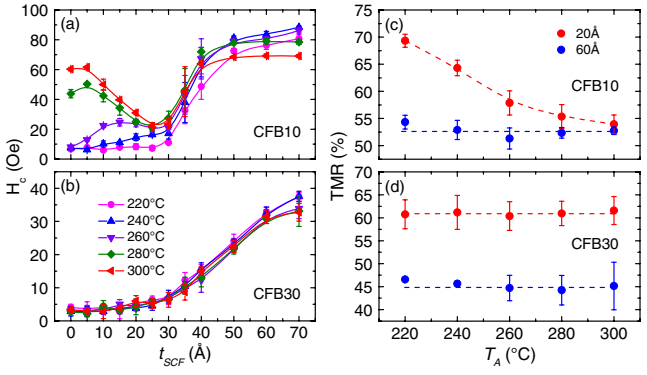

FIG. 3 (color online). (a) and (b) show the annealing temperature dependence of H_c on t_{SCF}; dependence of TMR on anneal temperature for (c) CFB10 and (d) CFB30 samples with $t_{SCF} =$ 20 [red (medium gray) circle] and 60 Å [blue (dark gray) circle] (the dashed lines are guides to the eye).

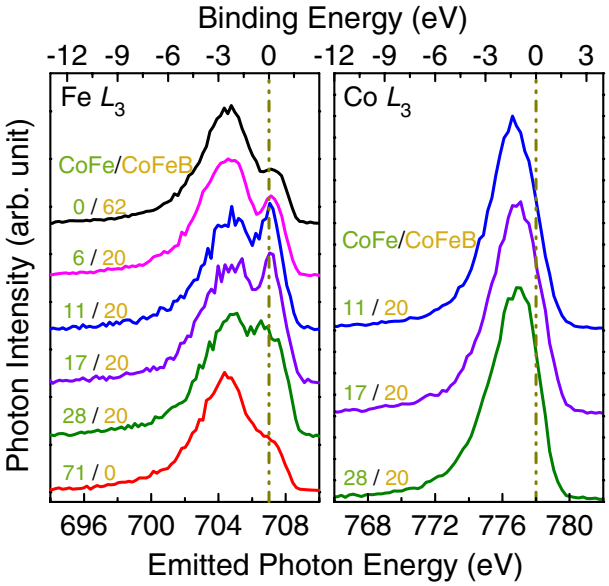

FIG. 4 (color online). Fe L_3 and Co L_3 XES spectra as a function of the SCF thickness for 50 Ta/18 Al_2O_3/[t_{SCF} SCF/20 CFB20], or 71 $Co_{70}Fe_{30}$, or 62 CFB20/10 $A1_2O_3$. The thicknesses of CoFe (CoFeB) are shown in green (orange). The Fe and Co $2p_{3/2}$ binding energies relative to the Fermi level are taken to be 707 eV and 778 eV, as indicated by the dark-yellow dashed-dotted lines.

alloys the TMR is much higher for the 20 Å amorphous as compared to the 60 Å crystalline SCF layer. Only for the thinner CFB10 alloy is any significant variation in TMR with T_A observed. In this case the TMR decreases on annealing to the value found for thick SCF layers, which are crystalline as deposited.

To understand whether the higher TMR of the amorphous SCF layers arises from changes in the bulk electronic structure of this layer, density functional electronic states were calculated for both crystalline (a bcc random solid solution) and amorphous structures of $Co_{70}F_{30}$. These calculations reveal substantial differences in the band structure of crystalline and glassy forms of *bulk* CoFe alloys, but a *decreased* spin polarization of the electrons at the Fermi energy, inconsistent with our results [22].

To explore whether the SCF-alumina interface electronic structure might be responsible for the enhanced TMR, x-ray emission spectroscopy (XES) was used to probe the density of filled electronic states at the buried Al_2O_3/SCF interface [23] in specially prepared structures of the form, 50 Ta/18 Al_2O_3/t_{SCF} SCF/20 CFB20($= Co_{56}Fe_{24}B_{20}$)/10 Al_2O_3 in which t_{SCF} was varied across a single wafer. The measured spectra are shown in Fig. 4, where the valence band binding energies relative to E_F are indicated. The broad, featureless Co spectra are similar to those previously found in bulk Co and in Co/Cu multilayers [23]. However, the Fe spectra show a feature near E_F whose intensity is significantly increased in the thickness range where we observed the SCF to be amorphous. Moreover, since the intensity of this feature is strongest for the thinnest SCF layers and this feature is weak in thick CFB20 layers, we conclude that this feature results from modifications to the electronic structure at the Al_2O_3/SCF interface.

Small changes in the atomic structure at the interface between a tunnel barrier and the magnetic electrodes can give rise to significant changes in the interface density of states and hence the spin-dependent tunneling conductance [24]. Therefore, it may not be surprising that whether the structure of the SCF layer is amorphous or crystalline strongly influences the TMR. Moreover, the XES strongly indicates both that the interface electronic structure is significantly altered compared to the bulk and that the Fe states play a dominant role. We have explored variations in the composition of the SCF layer from pure Co to pure Fe and find the highest TMR values for amorphous SCF layers with compositions near $Co_{70}Fe_{30}$. It could be that the chemical bonding at the SCF interface with alumina is important [25]. Stronger bonding with oxygen is expected for Fe as compared to Co at the alumina interface from bond energy considerations and we speculate that this difference could be accentuated when the ferromagnetic electrode is in an amorphous compared to a crystalline state due to atomic relaxation.

In summary, we find that thin CoFe films, sandwiched between two conventional amorphous materials, undergo an amorphous to crystalline transition at a critical thickness of ~25–30 Å. The amorphization of CoFe is accompanied by a significant enhancement of the tunneling magnetoresistance and increase of the Fe 3*d* density of states at the Fermi level. We postulate that these changes are related to the modification of interfacial bonding at the alumina-CoFe interface.

We thank Leslie Krupp for help with TEM sample preparation and Jinghua Guo for help with the XES experiments which were carried out at the Advanced Light Source, Berkeley.

*To whom all correspondence should be addressed.
parkin@almaden.ibm.com

[1] A. L. Greer, Science **267**, 1947 (1995).
[2] H. A. Davies and M. R. J. Gibbs, in *Handbook of Magnetism and Advanced Magnetic Materials*, edited by H. Kronmüller and S. S. P. Parkin (Wiley, New York, 2007).
[3] D. Wang *et al.*, IEEE Trans. Magn. **40**, 2269 (2004).
[4] S. S. P. Parkin *et al.*, Nature Mater. **3**, 862 (2004).
[5] S. Yuasa *et al.*, Nature Mater. **3**, 868 (2004).
[6] S. Ikeda *et al.*, Appl. Phys. Lett. **93**, 082508 (2008).
[7] D. D. Djayaprawira *et al.*, Appl. Phys. Lett. **86**, 092502 (2005).
[8] P. V. Paluskar *et al.*, Phys. Rev. Lett. **100**, 057205 (2008).
[9] S. X. Huang, T. Y. Chen, and C. L. Chien, Appl. Phys. Lett. **92**, 242509 (2008).
[10] EELS studies were carried out using a JEOL 2010F STEM (200 keV field emission electron gun; energy resolution ~1.2 eV) using a high spatial resolution (~5 Å diameter) probe and a Gatan Infina 1000 spectrometer. No evidence for B diffusion into the SCF layer was found.
[11] H. Yang, S. H. Yang, and S. S. P. Parkin, Nano Lett. **8**, 340 (2008).
[12] C. T. Campbell, Surf. Sci. Rep. **27**, 1 (1997).
[13] J. Landes *et al.*, Phys. Rev. B **44**, 8342 (1991).
[14] S. Handschuh *et al.*, J. Magn. Magn. Mater. **119**, 254 (1993).
[15] U. Herr, Contemp. Phys. **41**, 93 (2000).
[16] G. Herzer, J. Magn. Magn. Mater. **294**, 99 (2005).
[17] J. F. Löffler, H.-B. Braun, and W. Wagner, Phys. Rev. Lett. **85**, 1990 (2000).
[18] H. R. Liu *et al.*, J. Magn. Magn. Mater. **267**, 386 (2003).
[19] M. Vopsaroiu *et al.*, J. Optoelectron. Adv. Mater. **7**, 2713 (2005).
[20] E. Kita *et al.*, Appl. Phys. Lett. **88**, 152501 (2006).
[21] M. Hu, S. Noda, and H. Komiyama, J. Appl. Phys. **93**, 9336 (2003).
[22] L. Gao *et al.*, Appl. Phys. Lett. (to be published).
[23] A. Nilsson *et al.*, Phys. Rev. B **54**, 2917 (1996).
[24] E. Y. Tsymbal *et al.*, Prog. Mater. Sci. **52**, 401 (2007).
[25] C. Kaiser *et al.*, Phys. Rev. Lett. **94**, 247203 (2005).